GEOMORPHOLOGIC MAP OF THE SOUTH BELET REGION, TITAN.

A. M. Schoenfeld[1], M.J. Malaska[2], R.M.C. Lopes[2], M. Florence[2], T. Verlander[3], D.A. Williams[4], S.B.D. Birch[5], A.G. Hayes[5]

[1]Department of Earth, Planetary, and Space Sciences and the Institute of Planets and Exoplanets, University of California, Los Angeles, CA 90095-1567, USA. [2]Jet Propulsion Laboratory / California Institute of Technology, 4800 Oak Grove Drive, Pasadena, CA 98109. [3]University of Oklahoma, School of Civil Engineering and Environmental Science, Norman, Oklahoma. [4]School of Earth and Space Exploration, Arizona State Univeristy, Tempe, AZ 85281. [5]Department of Astronomy, Cornell University, Ithaca, NY 14850.

Introduction. The arrival of the Cassini-Huygens mission revealed Titan to be a geologically complex world, one characterized by channels [1,2], mountains [3-5], dune fields [6,7], lakes and seas [8-10], putative cryovolcanism [11,12], and other strikingly terrestrial features. Here we describe our mapping of Titan's South Belet region and associated geomorphological terrain units. This region spans the equatorial and mid-latitude region of the moon's southern hemisphere; our mapping thus characterizes the type and extent of terrains and geological processes typical of this locale. This mapping work is a continuation of the detailed global mapping effort introduced in Malaska et al. (2016) and continued on in Lopes et al., (2019).

Geologic Setting. The South Belet region (Fig. 1) extends from longitude 60°W to 120°W (+W coordinates) and from latitude 60°S to 0°, spanning both equatorial and mid-latitude regions. The areal extent of this region amounts to 9.5×10^6 km^2, or roughly about 11.32 % of Titan's surface. The region most notably contains the Belet Sand Sea, located on Titan's trailing hemisphere between 30°S and 25°N latitude and 65° and 150° W longitude, and is in a topographically low basin approximately -600 m in elevation [15]. Belet is the largest sand sea on Titan, with an estimated area of 3.3 ± 0.6 million km^2 and estimated sand volume of 610,000 to 1,270,000 km^3 [16].

Mapping Technique. We used Cassini's Synthetic Aperture Radar (SAR) data as our basemap, following the procedure described in Malaska et al. (2016). We distinguished between discrete terrain units and classes based on radar backscatter and overall morphology. Secondary datasets such as microwave emissivity, topography, and infrared reflectance to provide additional constraints on our terrain assignment. We mapped at a spatial scale of 300 m/pixel, which corresponded to a map scale of 1:800,000. Mapping was only done in areas covered with high resolution SAR swaths. The completed detailed map for the South Belet region is presented in Figure 2.

Description of Map Units. As for with the Afekan Crater region, the four major terrain classes are: craters, hummocky/mountainous, plains, and dunes [13]. Each terrain class was further subdivided into terrain units by characteristic morphology (border shape, texture, and general appearance) and radar backscatter. In general, radar backscatter is broadly classified as "high", "medium", "low", and in some cases as "variable". There are two terrain units that were not included in Malaska et al. (2016) but that were identified in our mapping of South Belet. We discuss them below.

Bright Alluvial Plains. The bright alluvial plains (*pah*) are radar bright, triangular shaped features typically found at the terminus of observable channel structure. These features have sharp to diffuse boundaries, with backscatter tending to decrease away from the apex of the triangle. These regions have low emissivity, much lower than other plains units like variable (*pfv*), undifferentiated (*pul*), and scalloped (*psv*). In some cases, the *pah* unit appears as radiometrically cool as the mountain/hummocky units. These features are interpreted as alluvial deposits of high backscatter materials emplaced by fluvial activity. Alluvial fans are evidence of either past or ongoing sediment transport, and the similarity of Titan's alluvial fans to those on Earth suggests similar underlying physical processes yet very different fluid and sediment compositions. [17]

Pitted Hummocky. Pitted hummocky terrain (*hpm*) units are high-backscatter regions with rounded boundaries with uniform to lumpy internal textures but are different in that they are "pitted" by dark circular features 1 to 6 km in diameter. A pitted hummocky feature maybe be partially or completed marked by these dark features. The microwave emissivity is the same of that as hummocky terrain unit (*hh*), and the SARTopo is consistent with these being locally elevated terrains. Similar features of this specific morphology, assumed to be depressions or pits, were first identified by Lopes et al. (2007) within Cassini's T8 swath. We interpret this terrain as highland areas of ancient crust and interpret the dark quasi-circular features within these exposures as dunes sands that have been deposited into pre-existing, circular depressions in the crustal ice. We hypothesize that these pits may have formed as a result of the removal of methane (either from outgassing or the retreat of a ground reservoir) in the near surface or formed as a result of the dissolution of soluble organics in an otherwise icy matrix.

In addition to the introduction of two new terrain units, South Belet similarly lacks several terrain units identified in Afekan. There is only one identified crater in South Belet and it is unnamed; we identify 4 crater-like features with potential impact origins as well, but they are insufficiently resolved to confidently describe as such. South Belet is likewise deficient in the "labyrinth" and "sharp edge depression" terrain units described in Malaska et al. (2016), suggesting either that the processes behind these units has not taken place in this area, or that they have since been completely eroded/buried.

Geologic Synthesis. Much like in the case of the Afekan region, our mapping shows that plains are the dominant class of terrain unit in South Belet, comprising 46.63% of the mapped area. Unlike Afekan, the dunes closely rival the dominance of plains, making up 43% of the mapped area. This is most likely a bias caused by lack of SAR coverage beyond South Belet's equatorial belt, underrepresenting the plains units that are more likely to be found south of the 30-degree latitude line. At the same time, South Belet hosts a large portion of the Belet Sand Sea, so it is reasonable to expect a larger representation of the dune units. The next prominent unit in the region following dunes are the mountains/hummocky terrains (10.36%), and finally, crater terrain units (0.01%).

Conclusion. The introduction of two new units, "bright alluvial plains" and "pitted hummocky", are necessary to capture the full range of morphologies seen in South Belet, and likewise indicate a morphological departure from Afekan. However, analysis of our geomorphological mapping results for South Belet is consistent with the narrative of Titan's equatorial and mid-latitudes being dominated by organic materials that have been deposited and emplaced by aeolian activity. This is similarly the conclusion we arrived at through our mapping and analysis of the Afekan region. Lastly, the applicability of the terrain units conceived of and applied to our mapping of the Afekan region to our mapping of South Belet suggests latitudinal symmetry in Titan's surface processes and their evolution.

References: [1] Barnes et al. (2007), *JGR*, 112, E11006. [2] Lorenz et al. (2008), *Planet. Space Sci.*, 56, 1132-1144. [3] Radebaugh et al. (2007), *Icarus*, 192, 77-91. [4] Cook-Hallet et al. (2015), *JGR Planets*, 120, 1220-1236. [5] Liu et al. (2016), *Icarus*, 270, 14-29. [6] Lorenz et al. (2006), *Science*, 312, 724–727. [7] Radebaugh et al. (2008), *Icarus*, 194, 690-703. [8] Stofan et al. (2007), *Nature*, 445, 61-64. [9] Brown et al. (2008), *Nature*, 445, 607-610. [10] Hayes et al. (2008), *Geophys. Res. Lett.*, 35, L09204. [11] Lopes et al. (2013), *JGR Planets*, 118, 1-20. [12] Le Corre et al. (2009), *Planet. Space Sci.*, 54, 870-829. [13] Malaska et al. (2016), *Icarus*, 270, 130-161. [14] Lopes et al. (2019), *Nature Astronomy*, 575, 426-427. [15] Lorenz et al. (2013), *Icarus*, 225, 367-377. [16] Le Gall et al. (2011), *Icarus*, 213, 608-624. [17] Birch et al. (2016), *Icarus*, 270, 238-247.[18] Lopes et al. (2007), *Icarus*, 186, 395-412. [19] Seignovert et al. (2019), *LPSC* abstract, 2132.

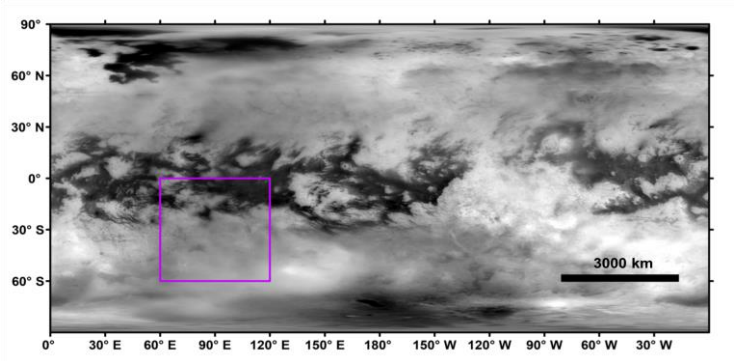

Figure 1. Global context of the South Belet region (marked in purple) on an ISS mosaic [19].

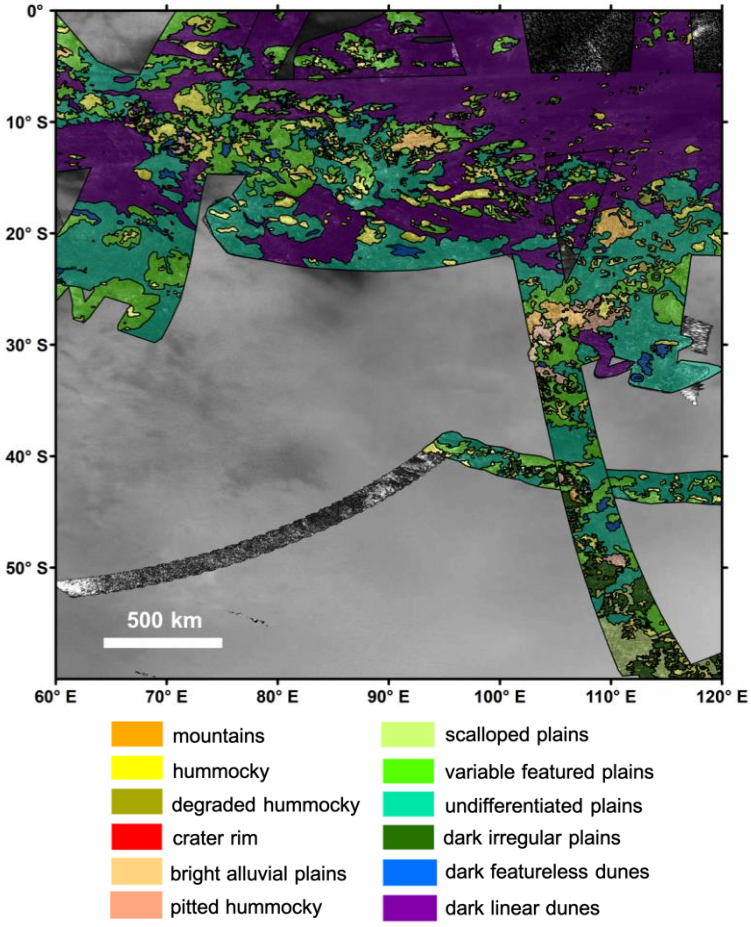

Figure 2. South Belet region geomorphogic map and terrain unit legend.